Reprinted from JOURNAL OF COMPUTATIONAL PHYSICS
All Rights Reserved by Academic Press, New York and London

Vol. 110, No. 2, February 1994
Printed in Belgium

Fire-Driven Flows in Enclosures

K. B. MCGRATTAN, R. G. REHM, AND H. R. BAUM

National Institute of Standards and Technology, Gaithersburg, Maryland 20899

Received February 2, 1993

A two-dimensional Boussinesq model describing heat-driven, buoyant convection in a polygonal enclosure is presented. The hydrodynamic model is based on the time-dependent Navier–Stokes equations with constant viscosity and thermal conductivity; no turbulence model or other empirical parameters are introduced. The polygonal domain is mapped via a numerical Schwarz–Christoffel transformation onto a rectangle, where the equations of motion are written in terms of the vorticity and stream function. An alternating direction implicit (ADI) difference scheme, second-order in space and first-order in time, is used to integrate the evolution equations, and a standard elliptic solver is used to solve the Poisson equation for the stream function. Computational results which are of interest to the fire research community are presented.

I. INTRODUCTION

The work described in this paper is part of an ongoing effort among fire researchers to develop models for assessing the impact of fire upon buildings and property. The study of fire dynamics requires consideration of materials, combustion, heat transfer, and fluid dynamics [1]. However, due to the wide variation of length and time scales and the large number of chemical and thermodynamic components in the problem, comprehensive models of fire behavior do not exist. Here we restrict our attention to fire-driven gaseous transport, avoiding serious modeling of the chemical reactions and thermal radiation in the neighborhood of the combustion zone. For our purposes, the fire serves as a source of buoyancy which induces large-scale mixing of air and combustion products, forming a plume which can persist as an organized structure over length scales ranging from centimeters to tens of meters in buildings and building complexes [2, 3]. Our objective is to develop the machinery necessary to model room fire phenomena without the use of subgrid turbulence models. To do this, we must approximately resolve internal and mixing boundary layers for flows whose Reynolds numbers are on the order of 10^5, a typical value for room fires. Unfortunately, to achieve these levels of resolution we are for the time being restricted to two-dimensional computations.

An additional difficulty in modeling enclosure fires is the presence of building elements such as windows, doorways, and stairwells which increase the complexity of the computations. In other areas of CFD, such as aerodynamics, calculations of the steady-state flow over aircraft have routinely required the use of sophisticated grid-generating techniques. In fire research, however, the study of fluid flow in more complicated domains is a more recent activity. Unfortunately, many of the techniques developed by the CFD community for solving flow equations on non-rectangular grids are not applicable to problems in fire research because they are designed to find steady-state, not transient, solutions, and they emphasize grids of more generality than required in the fire context.

In this paper we describe an algorithm which solves the time-dependent Navier–Stokes equations in the Boussinesq approximation for two-dimensional, polygonally shaped regions. We also demonstrate its usefulness in simulating phenomena such as gravity currents and backdrafts which are of interest to the fire research community.

II. HYDRODYNAMIC MODEL

We consider a thermally expandable ideal gas of constant viscosity and thermal conductivity which is driven by a prescribed heat source. The equations governing the motion of this fluid, based on the analysis of Rehm and Baum [3], are

$$\frac{\partial \rho}{\partial t} + \nabla \cdot \rho \mathbf{u} = 0 \tag{1}$$

$$\rho\left(\frac{\partial \mathbf{u}}{\partial t} + \mathbf{u}\cdot\nabla\mathbf{u}\right) + \nabla p - \rho\mathbf{g} = \mu\left(\frac{4}{3}\nabla(\nabla\cdot\mathbf{u}) - \nabla\times\boldsymbol{\omega}\right) \tag{2}$$

$$\rho c_p\left(\frac{\partial T}{\partial t} + \mathbf{u}\cdot\nabla T\right) - \frac{dp_0}{dt} = q + \kappa\nabla^2 T \tag{3}$$

$$p_0(t) = \rho\mathscr{R}T, \tag{4}$$

where ρ is the density, $\mathbf{u}$ is the velocity, $\boldsymbol{\omega}$ is the vorticity, $\mathbf{g}$ is the acceleration of gravity, μ is the dynamic viscosity, κ is

0021-9991/94 $6.00

the thermal conductivity, q is the spatially and temporally prescribed heat source, c_p is the constant-pressure specific heat, $\mathscr{R}$ is the effective gas constant, and T is the temperature. The specific heat is related to the gas constant by the equation

$$\mathscr{R} = \frac{\gamma - 1}{\gamma} c_p, \tag{5}$$

where γ is the ratio of specific heats c_p/c_v. The pressure p may be written as the sum of a background pressure $p_0(t)$, a hydrostatic pressure p_h, and a thermally induced pressure perturbation $\tilde{p}$.

We wish to reformulate these equations to describe the large-scale motion of the fluid away from the combustion zone. We start by noting that the velocity vector $\mathbf{u}$ can always be decomposed into a solenoidal field $\mathbf{v}$ plus an irrotational flow derived from a potential flow ϕ,

$$\mathbf{u} = \mathbf{v} + \nabla\phi, \tag{6}$$

where $\nabla \times \mathbf{v} = \boldsymbol{\omega}$ and $\nabla \cdot \mathbf{v} = 0$. The solenoidal field $\mathbf{v}$ is largely responsible for the motion of the smoke and hot gases transported far from the combustion zone [4], while the irrotational flow $\nabla\phi$, which is related to the heat source through the equation

$$p_0(t)\nabla^2\phi + \frac{1}{\gamma}\frac{dp_0}{dt} = \frac{\gamma - 1}{\gamma}(q + \kappa\nabla^2 T) \tag{7}$$

is only of importance in the combustion zone. Also, the net radiative emission from the fire can usually be subtracted from the chemical heat release, yielding a net heat release represented by the term q. The gases outside of the combustion zone are essentially transparent to infrared radiation which dominates the radiant emission from fires.

If we assume that the average enclosure pressure $p_0(t)$ is constant, and that, away from the heat source, the density is only slightly perturbed from its ambient value (i.e., $\rho = \rho_0(1 + \beta\tilde{\rho})$ for $\beta \ll 1$), then we may combine Eqs. (1) and (7) into an evolution equation for the density perturbation by making the Boussinesq approximation. In nondimensional form, this equation can be written

$$\frac{\partial\tilde{\rho}}{\partial t} + \mathbf{v}\cdot\nabla\tilde{\rho} = -q + \frac{1}{\mathrm{Re\,Pr}}\nabla^2\tilde{\rho}. \tag{8}$$

Note that all references to the velocity potential ϕ have been eliminated and thus the fluid may be thought of as incompressible. All lengths are relative to the enclosure height H, and the velocity is relative to a characteristic velocity V which is related to the magnitude of the heat source through the relation

$$V = \left(\frac{q_0 g}{\rho_0 c_p T_0}\right)^{1/3}.$$

The heat source strength q_0 is written in units of energy per unit time per unit length for the two-dimensional problem. The relative density difference β is related to the characteristic velocity through a Froude scaling $\beta = V^2/gH$. The Reynolds number $\mathrm{Re} = VH\rho_0/\mu$, and the Prandtl number $\mathrm{Pr} = c_p\mu/\kappa$.

The same set of assumptions may be applied to Eq. (2), and we write it as an evolution equation for the solenoidal velocity $\mathbf{v}$ in the Boussinesq approximation

$$\frac{\partial\mathbf{v}}{\partial t} + \boldsymbol{\omega}\times\mathbf{v} + \nabla\hat{p} - \tilde{\rho}\mathbf{g} = -\frac{1}{\mathrm{Re}}\nabla\times\boldsymbol{\omega}. \tag{9}$$

The term $\hat{p}$ is the nondimensionalized form of the reduced pressure $\tilde{p} + \rho_0 v^2/2$, and $\mathbf{g}$ is of unit magnitude. Away from the combustion zone, Eqs. (8) and (9) are an excellent approximation to the equations of motion for hot gas and smoke transport. Indeed, these equations are the basis of the salt experiments used as a physical analog of smoke movement in buildings [5].

III. NUMERICAL METHOD

Because we are interested in two-dimensional, polygonal geometries but wish to maintain the structure and efficiency of earlier algorithms, we have chosen to transform the spatial coordinates of the flow equations using a conformal map of the physical domain onto a rectangle. The conformality of the transformation allows us to retain the fast Poisson solver for Eq. (12) below which speeds up the computations considerably. The physical domain may be taken as any simply connected polygon whose vertices do not extend to infinity. This polygon is mapped conformally onto a rectangle whose aspect ratio is dependent on the shape of the polygon. A description of the Schwarz-Christoffel mapping package SCPACK may be found in [6]. For convenience, we write Eqs. (8) and (9) in terms of the scalar vorticity ω and the stream function ψ,

$$J\frac{\partial\tilde{\rho}}{\partial t} + \mathbf{v}\cdot\nabla\tilde{\rho} = -q + \frac{1}{\mathrm{Re\,Pr}}\nabla^2\tilde{\rho} \tag{10}$$

$$J\frac{\partial\omega}{\partial t} + \mathbf{v}\cdot\nabla\omega - \nabla\times\tilde{\rho}\mathbf{g} = \frac{1}{\mathrm{Re}}\nabla^2\omega \tag{11}$$

$$\nabla^2\psi = -J\omega, \tag{12}$$

where $J = \partial(x, y)/\partial(\xi, \eta)$ is the Jacobian of the mapping from the nondimensionalized physical coordinates (x, y) to the computational coordinates (ξ, η).

Equations (10)–(12) are a mixed parabolic/elliptic system of partial differential equations; i.e., the equations for the density and for the vorticity are parabolic, whereas that for the stream function is elliptic. The incompressible equations

of hydrodynamics are well known to have this mixed character. In [2] we used a lagged-diffusion leapfrog time-stepping scheme to solve the equations, but we found that this explicit method was severely restricted by the CFL condition imposed by the grid cells where the Jacobian is small, and it was also subject to instabilities. A simple Runge–Kutta second-order scheme was tried, and although it removed the instabilities of the earlier algorithm, it required twice as much CPU time as the leapfrog scheme. To incorporate both stability and efficiency in the model, we have chosen to use a simple version of the *alternating direction implicit* (ADI) method. Because of its good stability properties, we have decreased our typical CPU usage by a factor of five or six from those reported in [2].

A. *The Density Equation*

The density evolution equation in continuous form is the mass conservation equation minus the expression for the velocity divergence. Each of these two equations is approximated by central differences and then subtracted. Details of this procedure may be found in [2]. Note that within each rectangular cell, vector components are evaluated at the sides, scalar quantities at the center, and vorticity and the stream function at the corners. The ADI scheme advances in time the density perturbation of each cell $\tilde{\rho}_{ik}$ through the two-step process

$$J_{ik}\frac{\tilde{\rho}^{*}_{ik}-\tilde{\rho}^{n}_{ik}}{\delta t/2}+(u^{n}\,\delta_{\xi}-(\mathrm{Re}\cdot\mathrm{Pr})^{-1}\,\delta_{\xi\xi})\,\tilde{\rho}^{*}_{ik}$$
$$+(w^{n}\,\delta_{\eta}-(\mathrm{Re}\cdot\mathrm{Pr})^{-1}\,\delta_{\eta\eta})\,\tilde{\rho}^{n}_{ik}=-Jq^{n}_{ik}$$
$$J_{ik}\frac{\tilde{\rho}^{n+1}_{ik}-\tilde{\rho}^{*}_{ik}}{\delta t/2}+(u^{n}\,\delta_{\xi}-(\mathrm{Re}\cdot\mathrm{Pr})^{-1}\,\delta_{\xi\xi})\,\tilde{\rho}^{*}_{ik}$$
$$+(w^{n}\,\delta_{\eta}-(\mathrm{Re}\cdot\mathrm{Pr})^{-1}\,\delta_{\eta\eta})\,\tilde{\rho}^{n+1}_{ik}=-Jq^{n}_{ik},$$

where δ_{ξ} and $\delta_{\xi\xi}$ are the standard first- and second-order central difference approximations, and (u, w) are the components of the velocity vector $\mathbf{v}$ in the ξ and η directions, respectively. The nondimensional heat source at a point (ξ_i, η_k) is given by

$$q^{n}_{ik}=\tanh(\alpha t_n)\sqrt{\sigma_{\xi}\sigma_{\eta}/\pi^{2}}\;e^{-\sigma_{\xi}(\xi_i-\xi_c)^2-\sigma_{\eta}(\eta_k-\eta_c)^2},$$

where σ_{ξ}, σ_{η}, and the point (ξ_c, η_c) determine the spatial extent and the center of the heat source, respectively. At boundaries, the normal density gradient is specified by either an adiabatic $(\partial\tilde{\rho}/\partial n=0)$ or a cold-wall $(\tilde{\rho}=0)$ condition.

B. *The Vorticity Equation*

The vorticity equation may be differenced in either nonconservative or conservative form. The latter is preferable because it ensures nonlinear stability and complete compatibility between our earlier primitive variable formulation [2] and the vorticity-stream function formulation presented here. At internal grid cell nodes we have

$$J_{ik}\frac{\omega^{*}_{ik}-\omega^{n}_{ik}}{\delta t/2}+(\delta_{\xi}u^{n}-\mathrm{Re}^{-1}\,\delta_{\xi\xi})\,\omega^{*}_{ik}$$
$$+(\delta_{\eta}w^{n}-\mathrm{Re}^{-1}\,\delta_{\eta\eta})\,\omega^{n}_{ik}$$
$$+(\delta_{\eta}g^{(\xi)}-\delta_{\xi}g^{(\eta)})\,\tilde{\rho}^{n+1}_{ik}=0$$
$$J_{ik}\frac{\omega^{n+1}_{ik}-\omega^{*}_{ik}}{\delta t/2}+(\delta_{\xi}u^{n}-\mathrm{Re}^{-1}\,\delta_{\xi\xi})\,\omega^{*}_{ik}$$
$$+(\delta_{\eta}w^{n}-\mathrm{Re}^{-1}\,\delta_{\eta\eta})\,\omega^{n+1}_{ik}$$
$$+(\delta_{\eta}g^{(\xi)}-\delta_{\xi}g^{(\eta)})\,\tilde{\rho}^{n+1}_{ik}=0,$$

where $(g^{(\xi)}, g^{(\eta)})$ are the components of the normalized gravity vector and u and w are taken as averages of their values at the cell edges. The value of the vorticity at the boundary is not updated implicitly, but rather it is assigned a value after the stream function equation has been solved. Thus, there is a time-lag in the updating of the boundary vorticity, but this is not a great concern because the time-steps are relatively small [7]. The velocity at the boundary is determined by a no-flux condition and a no-slip condition.

C. *The Stream Function Equation*

At all interior cell corners, we have

$$(\delta_{\xi\xi}+\delta_{\eta\eta})\,\psi_{ik}=-J_{ik}\omega_{ik}$$

and $\psi=0$ on the boundary. We solve this equation using a standard elliptic PDE solver. The velocity components u and w are then computed at cell edges from the values of ψ at the corners

$$u_{ik}=\delta_{\xi}\psi_{ik};\qquad w_{ik}=-\delta_{\eta}\psi_{ik}.$$

The vorticity at the boundary is updated to be consistent with the stream function equation. For example, at the left boundary, $i=0$, we have

$$\frac{\psi_{1,k}+\psi_{-1,k}}{\delta\xi^{2}}=-J_{0k}\omega_{0k}$$

since $\psi_{0k}=0$. For no-slip boundary conditions, ψ is reflected evenly across the boundary, i.e., $\psi_{1,k}=\psi_{-1,k}$, thus

$$\omega_{0k}=-\frac{2\psi_{1k}}{J_{0k}\,\delta\xi^{2}}=\frac{2w_{1k}}{J_{0k}\,\delta\xi}.$$

The computation of vorticity at the boundary gives rise to a restriction on the time step analogous to that of the 1D heat equation. This will be discussed in the next section.

D. *Stability*

The vorticity and the density are updated at each time-step through an implicit scheme which requires the solution of a tridiagonal system of linear equations. To determine the stability requirements for the solution of this system, we consider the first step of the two-part vorticity time-step. Diagonal dominance of the kth row matrix is assured if

$$J_{ik}+\frac{\nu\,\delta t}{\delta\xi^2}>\frac{\delta t}{2}\left(\left|\frac{u_{i-1,k}}{2\,\delta\xi}+\frac{\nu}{\delta\xi^2}\right|+\left|\frac{u_{i+1,k}}{2\,\delta\xi}-\frac{\nu}{\delta\xi^2}\right|\right), \quad (13)$$

where $\nu=\mathrm{Re}^{-1}$. Assuming that $|u_{i-1,k}|\approx|u_{i+1,k}|\equiv U_{ik}$ the time-step must satisfy the inequality

$$\delta t<\frac{2J_{ik}\,\delta\xi^2}{U_{ik}\,\delta\xi-2\nu} \quad (14)$$

to achieve diagonal dominance [7]. Note that if $U_{ik}\,\delta\xi-2\nu<0$, then Eq. (13) is satisfied. The time-step restriction for the other tridiagonal systems which must be solved are also of this form. This stability criterion points out the severe limitation placed on the time-step when considering geometries in which there exist regions where the Jacobian approaches zero and the velocity is large. Note that in a stagnation region, this restriction is much less important.

In addition to the above stability criteria, for no-slip boundary conditions there is an additional constraint on the time-step size. This constraint is due to the imposition of vorticity at the boundary and is similar to the stability criterion of the 1D heat equation. Based on numerical tests of our own and by Peyret and Taylor [7], the restriction on δt is approximately

$$\delta t<\frac{2J\,\delta\xi^2}{\nu}. \quad (15)$$

This condition is less of a restriction for our work because our aim is to compute with the largest Reynolds number that a particular grid geometry will allow, in which case the time-step established by Eq. (14) is the limiting condition on the time-step rather than Eq. (15).

IV. RESULTS

In this section samples of results generated using a code implementing the algorithm described above are presented and discussed. The results represent some problems of interest to scientists concerned with enclosure fires. The computations typically consist of about half a million grid cells, requiring up to 100 Mb of memory and up to 30 h of CPU time on a high-end workstation.

A. *The Trench Effect*

Fires in buildings involve the transport of heat and mass by gravity-induced or buoyant convection. Generally, this convection occurs in rectangular enclosures where the direction of gravity is parallel to the walls. However, the enclosure may be sloped relative to gravity. A very important example of a fire in a sloped enclosure was the devastating fire in the King's Cross underground station in England in 1987, where there was significant loss of life as well as property damage. Numerical simulation of this fire uncovered an unexpected phenomenon which caused a very rapid spread of the fire and led to much of the devastation [8, 9]. This phenomenon was termed the trench effect and caused some controversy during investigations of the King's Cross fire in England. The phenomenon was ultimately confirmed by experiments and additional simulation, but transient aspects of the fire simulation are still of interest.

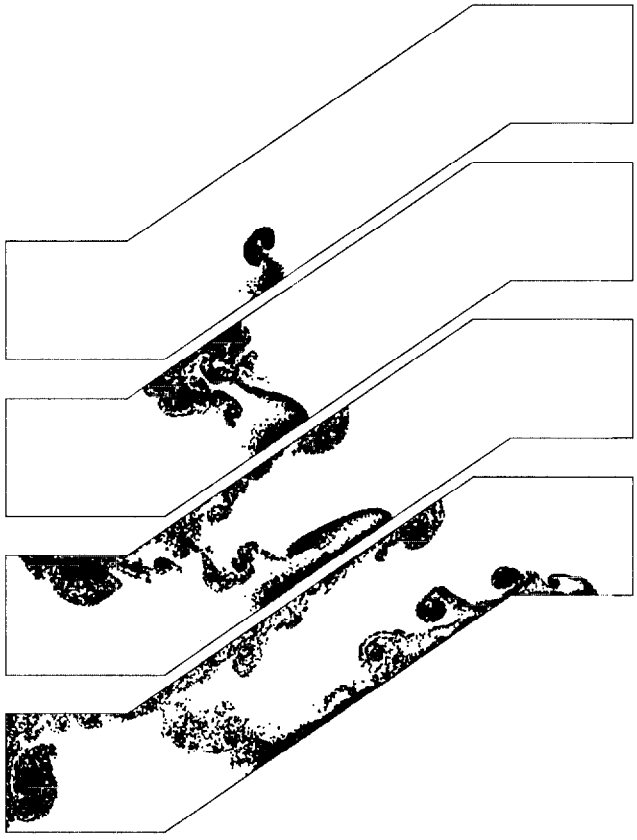

FIG. 1. Simulation of fire in a stairwell demonstrating the trench effect. Shown are particles which are advected with the flow. Adiabatic, free-slip boundary conditions have been imposed. The Reynolds number is 40,000; the grid size is 1024×256.

We repeat here a computational experiment performed with a rectangular domain tilted 35° from the horizontal which is intended to model a stairwell [10]. The major difference in the present calculation is the addition of more realistic "landings" to the geometry. Figure 1 presents a time sequence for the flow generated in an enclosure by a heat source (fire) located near the base of the stairwell. The mesh size is 1024×256 (262,144 grid cells), the Reynolds number based on the height of the landings is 40,000; and adiabatic, free-slip boundary conditions (mimicking an inviscid flow at large scales) are imposed. In this figure, the plume rises, but it is bent back toward the lower landing. After the hot gases hit the ceiling, they progress both toward the back wall and up the ceiling toward the high end. However, the hot gases leaving the heat source are pinned along the floor and form a hot gas jet which progresses up along the floor, shedding hot gases near its front. This phenomenon we interpret as the trench effect.

B. *Backdrafts*

In Fig. 3, we present the flow induced by a fire in a small enclosure with a window. Initially, the small compartment is filled with hot air, the larger area with ambient. Then the imaginary window separating the fluids is broken, and the hot and cold air mix at the interface. This is a challenging computation because of the wide variation in grid cell size. The mesh size is 1024×256; thus every cell pictured in Fig. 2 contains 64 subcells.

For convenience, we write Eqs. (8) and (9). This resolution allows for a Reynolds number of 40,000, based on the height of the small room. Adiabatic, no-slip boundary conditions are imposed to permit comparisons with salt water experiments. The stability requirement (14) limits the average time-step size to 1.5×10^{-3} nondimensionalized time units, and the density plot of Fig. 3 is shown five time units after the rupturing of the window. We note that the vorticity of the escaping plume tends to pin the hot gas to the wall of the enclosure, a phenomenon which has been seen in actual fires where the flames and hot gases pour out of an enclosure opening and then spread rapidly up the side of the building. This type of fire scenario is of interest to those studying phenomena known as backdrafts [11]. These occur when a fire in a sealed compartment consumes most of the available oxygen and apparently dies out, but is then re-ignited when fresh air is allowed to flow into the room following the opening of a door or breaking of a window.

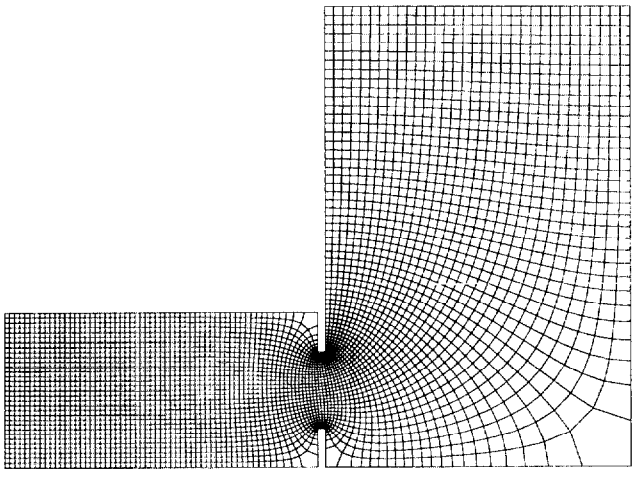

FIG. 2. A skeleton of the computational grid used for the backdraft simulations. This figure is mapped conformally onto a rectangle using the Schwarz–Christoffel mapping package SCPACK [6].

C. *Gravity Current*

Finally, we consider the flow induced by the introduction of salt water into a long rectangular tank filled with fresh water. As noted above, this type of experiment is often used to model the transport of smoke and hot gases along the ceiling of a long corridor of a building. The flow is an example of a general class of flows known as gravity currents, which arise in geophysical processes as well as in heating, ventilating and air conditioning (HVAC) applications [12]. Figure 4 displays a few profiles of a computed gravity current. Heavy fluid flows into the enclosure via a slot opening at the lower left, and the overflow is evacuated out of an equally sized opening at the upper right.

The equations of motion for the salt/fresh water mixture are exactly those given above, with the thermal conductivity analogous to the material diffusivity of the salt water, and the Prandtl number analogous to a Schmidt number. The analogy is not perfect because the Prandtl number for air is about 0.7, whereas the Schmidt number for salt water is on the order of several hundred. We can compute directly flows whose Schmidt numbers are on the order of one, and we can consider the special case where the Schmidt number is infinite, solving Eq. (10) in Lagrangian form (with density determined by initial salinity concentration and $q = 0$)

$$\frac{D\tilde{\rho}}{Dt} = 0. \tag{16}$$

We have compared our computational results using both forms of the density equation with the gravity current experiments of Chan, Zukoski, and Kubota [13], and have found that the results are insensitive to the size of the Prandtl/Schmidt number. In the experiments salt water is pumped into a long rectangular tank of square cross section at a specified rate. For the computation, we use a 16×1 rectangular enclosure (3072×192 cells). The Reynolds number for the computation (based on the enclosure height) is about 30,000. Figure 5 compares the head trajectories for

FIG. 3. Simulation of smoke pouring from a window. Shown are nondimensionalized contours of temperature. Adiabatic, no-slip boundary conditions have been imposed. The Reynolds number is 40,000; the grid size is 1024×256.

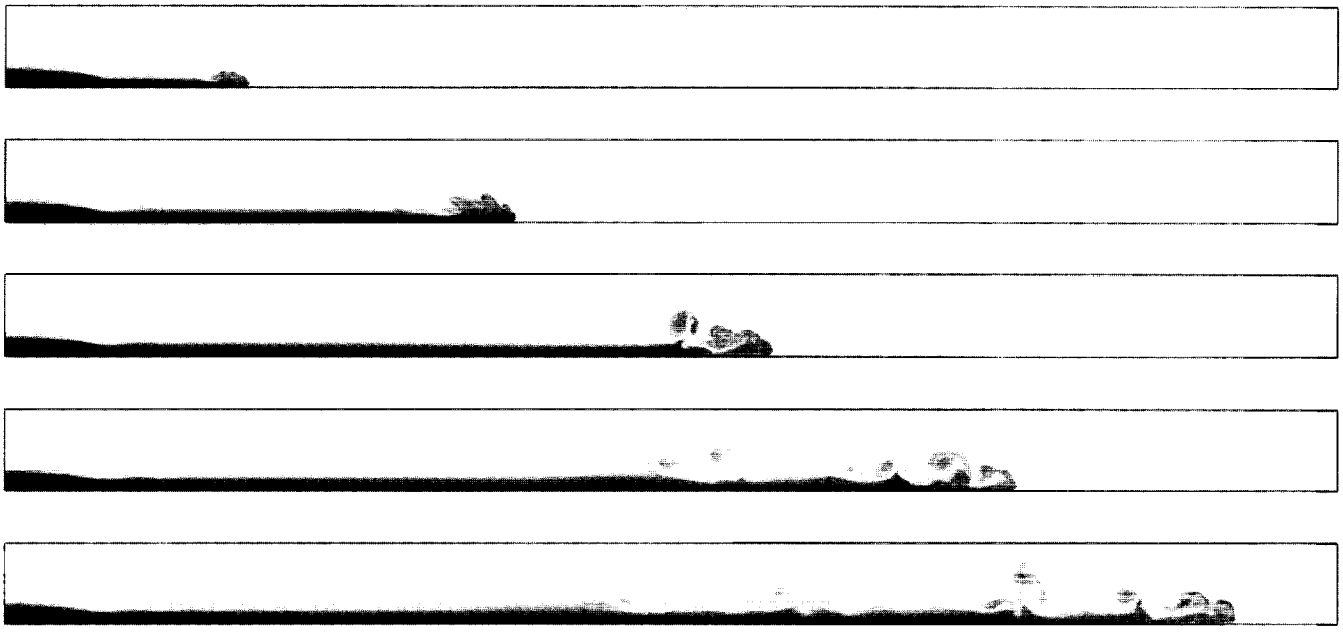

FIG. 4. A gravity current develops as heavy fluid is pumped into the channel at the lower left and evacuated at the upper right. Shown are nondimensionalized contours of density.

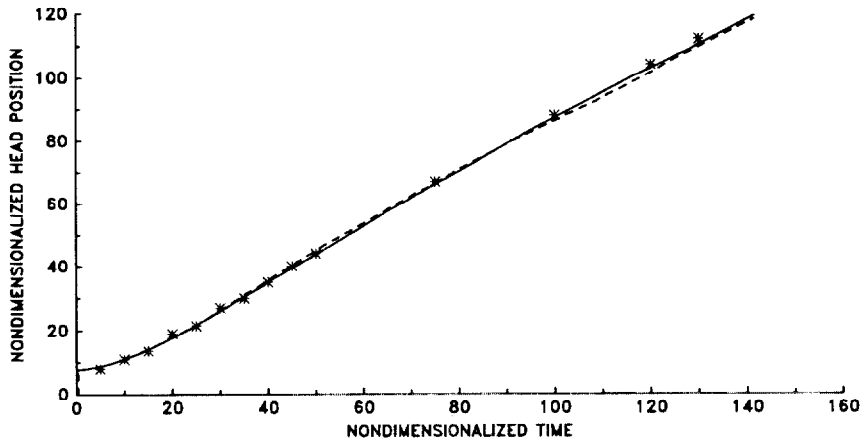

FIG. 5. A comparison of the gravity current trajectories for a nondiffusive computation (solid line), a diffusive computation (dashed line), and a salt water experiment (stars).

the experiment and the computation. The agreement between the computations and the experiment is excellent and gives us great confidence in the methodology.

V. CONCLUSION

The methodology outlined in this paper provides a solid foundation for the future study of smoke transport and other topics of interest in combustion and fire research. In several years time, we are confident that increased computing power will enable three-dimensional computations based on the ideas described here, as well as the inclusion of more realistic subgrid combustion models. Unfortunately, some of the techniques used for the 2D problem, namely the conformal mapping and the vorticity-stream function approach, become troublesome in 3D, but there are certainly other methods which can be applied. What is most valuable are the set of assumptions about the fire and fire-induced flow field which lead to a great simplification of the relevant equations.

REFERENCES

1. J. W. Lyons, "Fire," Scientific American Library (Freeman, New York, 1985).
2. K. B. McGrattan, R. G. Rehm, H. C. Tang, and H. R. Baum, NIST Internal Report, NISTIR 4831 (National Institute of Standards and Technology, Gaithersburg, MD, 1992).
3. R. G. Rehm and H. R. Baum, *J. Res. Nat. Bur. Stand.* **83** (3), 297 (1978).
4. H. R. Baum and B. J. McCaffrey, "Fire Induced Flow Field—Theory and Experiment," in *Fire Safety Science—Proceedings, Second International Symposium*, (Hemisphere, New York, 1989), p. 129.
5. K. D. Steckler, H. R. Baum, and J. G. Quintiere, "Salt Water Modeling of Fire Induced Flows in Multicompartment Enclosures," in *Twenty-First Symposium (International) on Combustion* (The Combustion Institute, Pittsburgh, PA, 1988), p. 143.
6. L. N. Trefethen, "SCPACK User's Guide," Numerical Analysis Report 89-2, (Department of Mathematics, Massachusetts Institute of Technology, Cambridge, MA, 1989).
7. R. Peyret and T. Taylor, *Computational Methods for Fluid Flow* (Springer-Verlag, New York, 1983).
8. S. Simcox, N. S. Wilkes, and I. P. Jones, *Fire at King's Cross Underground Station, 18th November 1987: Numerical Simulation of the Buoyant Flow and Heat Transfer*, Harwell Report AERE-G-4677 (Harwell Laboratories, England, 1988).
9. G. Cox, R. Chitty, and S. Kumar, *Fire Safety J.* **15**, 103 (1989).
10. R. G. Rehm, H. R. Baum, D. W. Lozier, H. C. Tang, and J. Sims, in *Third International Symposium on Fire Safety Science, The University of Edinburgh, Scotland, 1991*, p. 313.
11. C. M. Fleischmann, P. J. Pagni, and R. B. Williamson, *Fire Technol.*, to appear.
12. J. E. Simpson, *Gravity Currents in the Environment and the Laboratory* (Wiley, New York, 1987).
13. W. R. Chan, E. E. Zukoski, and T. Kubota, *Experimental and Numerical Studies on Two-Dimensional Gravity Currents in a Horizontal Channel* (Guggenheim Jet Propulsion Center, California Institute of Technology, Pasadena, CA, 1992).

Printed by Catherine Press, Ltd., Tempelhof 41, B-8000 Brugge, Belgium